Polyhedron 300 (2026) 118433

Contents lists available at ScienceDirect

Polyhedron

journal homepage: www.elsevier.com/locate/poly

From antioxidants to apoptosis: How chain length governs phthalocyanine biofunctionality

Dilek Bahar [a], H. Yasemin Yenilmez [b,*], Muazzez Derya-Andeden [c], Pınar Altin-Celik [c], Nilgün Güler [d]

[a] Genkök Genome and Stem Cell Center, Erciyes University, 38030 Kayseri, Türkiye
[b] Faculty of Science and Letters, Department of Chemistry, İstanbul Technical University, 34469, Maslak, Istanbul, Türkiye
[c] Faculty of Medicine, Medical Biology Department, Erciyes University, Melikgazi, Kayseri, Türkiye
[d] Kayseri University, Mustafa Çıkrıkçıoğlu Vocational School, Kayseri, Türkiye

ARTICLE INFO

Keywords:
Metallophthalocyanine
MTT
DLD-1
HT-29
Quantum yield
Antioxidant activity

ABSTRACT

In this study, tetra-substituted zinc and indium phthalocyanines with different chain lengths were synthesized. All compounds were characterized by FT-IR, ^{1}H NMR, MALDI-TOF, and UV–vis spectroscopy. The in vitro anticancer/cytotoxic properties of the compounds were investigated using 3-(4,5-dimethylthiazol-2-yl)-2,5-diphenyltetrazolium (MTT) assay in colorectal cancer cell lines (DLD-1 and HT29 cells). The effects of chain length and central metal atom on the cytotoxic properties of the phthalocyanine compounds were compared. Fluorescence quantum yields and lifetimes of the phthalocyanine derivatives were determined. Additionally, the singlet oxygen quantum yields of the quaternized phthalocyanine derivatives were determined. The antioxidant activities of the phthalocyanine derivatives were examined using 2,2-diphenyl-1-picrylhydrazyl (DPPH) assay. The phthalocyanine derivatives exhibited lower DPPH radical-scavenging activity (4.0–53.8%) than BHT (88.0%), indicating modest and compound-dependent cell-free radical-scavenging activity. The compounds were screened for cytotoxic and apoptotic effects against human colon cancer cell lines (DLD-1 and HT29) using MTT and Annexin V assays. The results showed that the compounds have antiproliferative and apoptotic effects against DLD-1 and HT29 cell lines. Overall, the derivatives exhibited distinct photophysical, cell-free radical-scavenging, and cell-line-dependent cytotoxic and apoptotic profiles. However, further mechanistic studies are required to determine whether these properties are functionally related.

1. Introduction

Phthalocyanines (Pcs) are important members of the tetrapyrrole family [1]. Their macrocyclic structure is composed of four iminoisoindole units and contains an 18-π electron conjugated system. The central cavity of the Pc ring can accommodate more than 70 different metal ions, providing considerable structural diversity and allowing their physicochemical and biological properties to be tuned through metal coordination [2]. Although structurally related to porphyrins, phthalocyanines are synthetic compounds and do not occur naturally, unlike biologically important porphyrin derivatives such as chlorophyll and hemoglobin. Initially developed mainly as dyes and pigments, they have attracted increasing scientific interest because of their distinctive optical, electronic, chemical, and biological characteristics [3–6]. Nevertheless, the poor solubility of unsubstituted derivatives remains an important limitation for many practical applications. Introducing suitable substituents onto the macrocyclic framework can improve solubility and, at the same time, reduce aggregation between the aromatic rings. Such structural modifications have therefore become an effective approach for tailoring their properties for different applications.

Metal-containing coordination systems are fundamental to many biological processes. For example, hemoglobin and myoglobin are involved in oxygen transport and storage, respectively, whereas chlorophyll plays a central role in photosynthesis. In each case, the biological function is closely related to the coordination of a metal ion within a pyrrole-based framework. The structural resemblance of phthalocyanines to these naturally occurring systems, together with their ability to coordinate a wide range of metal ions, has prompted considerable interest in their biological activity [7–10]. Changes in the central metal and peripheral substituents can substantially affect their interactions

* Corresponding author.
E-mail address: yenilmez@itu.edu.tr (H.Y. Yenilmez).

https://doi.org/10.1016/j.poly.2026.118433
Received 30 April 2026; Accepted 5 October 2026
Available online 6 October 2026
0277-5387/© 2026 Elsevier Ltd. All rights are reserved, including those for text and data mining, AI training, and similar technologies.

with biological systems, making structural modification an important strategy in the design of biologically active derivatives.

Cancer is a complex disease that develops through the uncontrolled proliferation of cells as a result of interactions between genetic and environmental factors [11]. It remains one of the leading aggregation in aqueous media of death worldwide, with pancreatic, colorectal, breast, gastric, lung, and prostate cancers among the most common forms [12]. Colorectal cancer is particularly important because its development is influenced by both genetic susceptibility and environmental factors. Lifestyle-related conditions, including an unhealthy diet, inadequate consumption of fruits and vegetables, smoking, alcohol use, and physical inactivity, can further increase the risk of disease [13]. Although chemotherapy and radiotherapy are widely used in the treatment of colorectal cancer, their effectiveness can be compromised by toxicity toward healthy tissues and the emergence of drug resistance. These limitations have increased the need for new therapeutic candidates with alternative mechanisms of action and improved biological profiles [14,15].

Metal-based compounds have attracted considerable attention in this context because their coordination environments, geometries, redox properties, and kinetic and thermodynamic characteristics can be readily modified. The discovery of the anticancer activity of cisplatin demonstrated the potential of metal complexes as therapeutic agents and opened an important field of research in medicinal chemistry. Despite its clinical success, cisplatin has several limitations, including reduced effectiveness against certain cancer types, the development of resistance, and serious side effects such as neurotoxicity, alopecia, and nausea [16,17]. Consequently, considerable effort has been devoted to identifying new metal-containing structures that can provide effective anticancer activity while overcoming some of the limitations associated with conventional agents.

Oxidative stress is another important factor associated with cellular damage and disease development. Reactive oxygen species (ROS) can arise from normal intracellular oxidation processes as well as from external factors such as air pollution, chemical exposure, and medical radiation [18]. When their production exceeds the capacity of the antioxidant defense system, these highly reactive species can damage cellular components. Antioxidants counteract this process by neutralizing reactive species and are generally classified as enzymatic or non-enzymatic. Catalase, superoxide dismutase, glutathione reductase, and glutathione peroxidase are among the major enzymatic antioxidants, whereas non-enzymatic antioxidants include naturally occurring molecules such as tocopherols (vitamin E), ascorbic acid (vitamin C), melatonin, uric acid, and polyphenols [19]. Synthetic antioxidants, including BHT, BHA, TBHQ, and PG, are also widely used in the food industry to delay oxidative deterioration and improve storage stability [20].

The search for new synthetic antioxidants has led to increasing interest in structurally diverse compounds, including phthalocyanine derivatives. Their antioxidant capacity has been evaluated by several complementary assays, and a number of studies have reported appreciable radical-scavenging activity [21–25]. Beyond their antioxidant behavior, the structural versatility of these macrocycles makes it possible to modify their biological activity through changes in peripheral substituents and the coordinated metal ion. This is particularly relevant to anticancer research, where both oxidative balance and interactions with cellular targets can influence the response of cancer cells.

At the same time, advances in nanomaterials and functional inorganic systems have broadened the possibilities for developing new approaches to cancer treatment and drug delivery. Carbon-based nanomaterials and related functional materials have received considerable attention because of their ability to enhance the delivery and biological performance of therapeutic agents and to influence the tumor microenvironment [26–28]. These developments underline the importance of controlling molecular structure, surface functionality, and physicochemical characteristics when designing new anticancer systems. Within this framework, metallophthalocyanines are particularly attractive because both the central metal ion and peripheral substituents can be systematically varied. Such modifications can influence solubility, aggregation, electronic structure, cellular interactions, and ultimately biological activity. These structural features may directly influence the biological behavior and cytotoxic activity of the derivatives, particularly under dark conditions.

Functionalized metallophthalocyanines containing aminoalkyl groups have been widely studied because the introduction of such groups can improve their solubility and provide a convenient site for further modification. For example, Gürsoy et al. reported Zn(II) and Co(II) phthalocyanines bearing dimethylaminoethylsulfanyl groups and their water-soluble quaternized derivatives [29]. Similarly, tetra-substituted titanyl phthalocyanines containing dimethylaminoethylsulfanyl groups and their quaternized analogues were reported by Arslanoğlu and Hamuryudan [30]. Bıyıklıoğlu et al. also reported zinc phthalocyanines bearing 2-[2-(dimethylamino)ethoxy]ethoxy substituents and their quaternized derivatives [31].

In the present study, the peripheral substituent was designed to combine thioether and ether functionalities within the same side chain, namely —S—(CH_2)n—O—CH_2CH_2—$N(CH_3)_2$. Two different spacer lengths (n = 2 and 6) were investigated, and both Zn(II) and In(III)Cl phthalocyanines were prepared together with their corresponding quaternized derivatives. Therefore, although amino-functionalized and quaternized phthalocyanines have been previously reported, the present work provides a systematic comparison of the effect of spacer length, central metal and quaternization within this specific thioether–ether-linked dimethylamino substituent. This structural approach also enabled the relationship between these modifications and the physicochemical and biological properties of the resulting phthalocyanines to be examined. Their antioxidant activities were evaluated using established assays, while their cytotoxic effects were examined by the MTT assay. Fluorescence quantum yields were also determined to investigate the effect of aliphatic chain length on the fluorescence properties of the derivatives. The biological experiments were conducted under dark conditions, with the aim of evaluating the direct, light-independent cytotoxic activity of the synthesized structures. Their effects on the viability of human colon cancer DLD-1 and HT29 cells were further examined, and apoptosis was assessed using the Annexin V assay. The results demonstrated that the synthesized derivatives exhibited both antiproliferative and apoptotic effects against the two colorectal cancer cell lines. In addition, the influence of aliphatic chain length and the central metal ion on antioxidant and cytotoxic responses was comparatively assessed. Taken together, these findings provide insight into the relationship between molecular structure and biological activity and highlight the potential of these phthalocyanine derivatives as promising candidates for further investigation in anticancer research.

2. Experimental

4-(2-hydroxyethylsulfanyl) phthalonitrile (**1**), 4-(6-hydroxyhexylsulfanyl) -1,2-dicyanobenzene (**2**), 2,9,16,23-tetrakis(2-hydroxyethylsulfanyl) phthalocyaninatozinc(II) (**3a**) and 2,9,16,23-tetrakis (6-hydroxyhexylsulfanyl) phthalocyaninatozinc(II) (**4a**) were synthesized according to the literature [32,33].

2.1. General procedures for indium phthalocyanine derivatives (*3b* and *4b*)

1 mmol dinitrile compound (**1**: 0.204 g or **2**: 0.260 g), 0.25 mmol indium (III) chloride (0.055 g) and DMF (1.5 mL) (2-dimethylaminoethanol for **2**) were stirred at 145 °C for 24 h under N_2. After cooling, the solid product was precipitated with methanol. The product was dissolved with a small amount of THF and precipitated in methanol. The precipitate that forms is filtered and purified by washing with methanol, acetone, and n-hexane.

2(3), 9(10), 16 (17), 23(24) -Tetrakis(2-hydroxyethylsulfanyl)phthalocyaninato(chloro)-indium(III) ***(3b):*** Yield: 116 mg (45%). ^{1}H NMR (500 MHz, DMSO-d_6) δ 8.39 (s, Ar—H, 8H), 7.94 (s, Ar—H, 4H), 5.20 (, OH, 4H), 4.22 (m, CH_2, 4H), 2.30 (m, CH_2, 4H). FT-IR, ν/cm^{-1}: 3040 (aromatic C—H), 2928–2870 (aliphatic C—H), 1348 (C—N), 1224 (C-O-C). MS *m/z* calculated $[M]^+$ 966.02; found 929.32 $[M\text{-}Cl]^+$. UV–Vis (DMF) λ_{max}/nm (log ε): 368 (4.78), 709 (5.16).

2(3), 9(10), 16 (17), 23(24) -Tetrakis(6-hydroxyhexylsulfanyl)phthalocyaninato(chloro)-indium(III) ***(4b):*** The product is purified by column chromatography on silica gel using THF. Yield: 152 mg (53%). ^{1}H NMR (500 MHz, DMSO-d_6) δ 7.71–7.54 (m, Ar—H, 12H), 4.36–4.35 (s, OH, 4H), 3.55–3.53 (m, CH_2, 16H), 3.00–2.94 (m, CH_2, 16H), 2.66–2.64 (m, CH_2, 8H), 1.93–1.88 (m, CH_2, 8H). FT-IR, ν/cm^{-1}: 3050 (aromatic C—H), 2928–2878 (aliphatic C—H), 1345 (C—N), 1222 (C-O-C). MS *m/z* calculated $[M]^+$ 1191.69; found 1155.30 $[M\text{-}Cl]^+$. UV–Vis (DMF) λ_{max}/nm (log ε): 382 (4.97), 723 (5.19).

2.2. Synthesis of 2-[2-(dimethylamino)ethoxy]ethyl/hexylsulfanyl-substituted phthalocyanine derivatives (5a-b)

0.113 mmol of phthalocyanine derivative (**3a**: 100 mg; **3b**: 109 mg) and 2-chloro-*N*,*N*-dimethylethylamine hydrochloride (98 mg, 0.678 mmol) were dissolved in 1 mL of toluene in a tube and then sodium hydride (5 mg, 0.208 mmol) was added. The reaction mixture was heated to 50 °C for 24 h. After the reaction mixture was cooled to room temperature, the toluene was removed under vacuum.

2(3), 9(10), 16 (17), 23(24) -Tetrakis -(2-[2-(dimethylamino)ethoxy]ethylsulfanyl)- phthalocyaninato zinc(II) ***(5a):*** The product was separated from the starting compound with low solubility by dissolving it with THF. The product was purified by washing with methanol, acetone, and n-hexane. Yield: 40 mg (30%). ^{1}H NMR (500 MHz, DMSO-d_6) δ 7.61–7.55 (s, Ar—H, 4H), 7.15–7.10 (s, Ar—H, 8H), 4.15 (br, CH_2, 16H), 2.18–2.13 (s, CH_3, 24H), 1.19–1.18 (br, CH_2, 16H). FT-IR, ν/cm^{-1}: 3045 (aromatic C—H), 2924–2868 (aliphatic C—H), 1350 (C—N), 1212 (C-O-C). MS *m/z* calculated $[M]^+$ 1164.37; found; 1165.47 $[M + H]^+$. UV–Vis (DMF) λ_{max}/ nm (log ε): 365 (4.63), 693 (5.15).

2(3), 9(10), 16 (17), 23(24) -Tetrakis -(2-[2-(dimethylamino)ethoxy]ethylsulfanyl)- phthalocyaninato(chloro)-indium(III) ***(5b):*** The product was separated from the starting compound with low solubility by dissolving it with THF. The product was purified by washing with methanol, acetone, and n-hexane. Yield: 52 mg (37%). ^{1}H NMR (500 MHz, DMSO-d_6) δ 8.39 (s, Ar—H, 8H), 7.94 (s, Ar—H, 4H), 3.96–3.93 (m, CH_2, 8H), 3.11–3.08 (m, CH_2, 8H), 2.57–2.53 (m, CH_2, 16H), 2.18 (s, CH_3, 24H). FT-IR, ν/cm^{-1}: 3040 (aromatic C—H), 2925–2878 (aliphatic C—H), 1386(C—N), 1094 (C-O-C). MS *m/z* calculated $[M]^+$ 1251.75; found 1251.85 $[M]^+$. UV–Vis (DMF) λ_{max}/nm (log ε): 342 (5.01), 687 (5.17).

2.3. Synthesis of 2-[2-(dimethylamino)ethoxy]hexylsulfanyl-substituted phthalocyanine derivatives (6a-b)

0.113 mmol of phthalocyanine derivative (**4a**: 125 mg; **4b**: 135 mg) and 2-chloro-*N*,*N*-dimethylethylamine hydrochloride (98 mg, 0.678 mmol) were dissolved in 1 mL of toluene in a tube and then sodium hydride (5 mg, 0.208 mmol) was added. The reaction mixture was heated to 50 °C for 24 h. After the reaction mixture was cooled to room temperature, the toluene was removed under vacuum.

2(3), 9(10), 16 (17), 23(24) -Tetrakis -(2-[2-(dimethylamino)ethoxy]hexylsulfanyl)- phthalocyaninatozinc(II) ***(6a):*** The product was purified by column chromatography on neutral alumina using THF. Yield: 55 mg (35%). ^{1}H NMR (500 MHz, DMSO-d_6) δ 9.24–9.17 (d, Ar—H, 8H), 8.09–8.07 (s, Ar—H, 4H), 3.46–3.41 (m, CH_2, 16H), 1.88 (s, CH_2, 8H), 1.62–1.43 (m, CH_2, 40H), 1.21 (s, CH_3, 24H). FT-IR, ν/cm^{-1}: 3055 (aromatic C—H), 2928–2875 (aliphatic C—H), 1345 (C—N), 1224 (C—O—C). MS *m/z* calculated $[M]^+$ 1391.29; found 1347.30 $[M\text{-}(CH_3)N]^+$. UV–Vis (DMF) λ_{max}/nm (log ε): 364 (4.75), 695 (5.18).

2(3), 9(10), 16 (17), 23(24) -Tetrakis -(2-[2-(dimethylamino)ethoxy]hexylsulfanyl)- phthalocyaninato(chloro)-indium(III) ***(6b):*** Yield: 80 mg (48%). ^{1}H NMR (500 MHz, DMSO-d_6) δ 8.47 (s, Ar—H, 4H), 7.31–7.16 (s, Ar—H, 8H), 2.74–2.73 (s, CH_2, 16H), 2,26–2.18 (m, CH_3, 24H), 2.14–1.88 (m, CH_2, 16H), 0.84–0.74 (m, CH_2, 24H). FT-IR, ν/cm^{-1}: 3045 (aromatic C—H), 2928–2875 (aliphatic C—H), 1383(C—N), 1101 (C—O—C). MS *m/z* calculated $[M]^+$ 1476.18 found; 1436.46 $[M\text{-}Cl\text{-}3H]^+$. UV–Vis (DMF) λ_{max}/nm (log ε): 350 (4.99), 689 (5.05).

2.4. Synthesis of quaternary phthalocyanine derivatives (7a-b, 8a-b)

45 μmol phthalocyanine derivative (**5a**: 53 mg; **5b**: 56 mg; **6a**: 63 mg; **6b**: 66 mg) was dissolved in 3 mL of DMF. After iodomethane (122 mg, 857 μmol) was added to the solution, it was stirred for 72 h at 50 °C in the dark. After the solution was precipitated with chloroform, it was washed with chloroform and n-hexane, respectively.

Compound ***7a:*** Yield: 49 mg (66%). ^{1}H NMR (500 MHz, DMSO-d_6) δ 8.85–8.78 (m, Ar—H, 4H), 8.10–8.00 (m, Ar—H, 8H), 5.01 (s, CH_2, 16H), 3.66–3.09 (m, CH_2, 16H), 2.54 (s, CH_3, 36H). FT-IR, ν/cm^{-1}: 3060 (aromatic C—H, 2925–2874 (aliphatic C—H), 1375 (C—N), 1214 (C-O-C). UV–Vis (DMF) λ_{max}/nm (log ε): 364 (4.68), 694 (5.16).

Compound ***7b:*** Yield: 50 mg (64%). ^{1}H NMR (500 MHz, DMSO-d_6) δ 7.69–7.59 (m, Ar—H, 12H), 2.73–2.68 (s, CH_2, 16H), 1.92–1.87 (s, CH_2, 16H), 1.39–1.36 (s, CH_3, 36H). FT-IR, ν/cm^{-1}): 3050 (aromatic C—H), 2928–2875 (aliphatic C—H), 1364 (C—N), 1098 (C-O-C). UV–Vis (DMF) λ_{max}/nm (log ε): 369 (4.76), 704 (5.15).

Compound ***8a:*** Yield: 60 mg (71%). ^{1}H NMR (500 MHz, DMSO-d_6) δ 9.18 (s, Ar—H, 8H), 8.48 (s, Ar—H, 4H), 3.51–3.48 (m, CH_2, 16H), 3.18–3.17 (m, CH_3 and CH_2, 48H), 1.22 (m, CH_2, 24H), 0.84 (m, CH_2, 24H). FT-IR, ν/cm^{-1}: 3045 (aromatic C—H), 2928–2875 (aliphatic C—H), 1385 (C—N), 1225 (C-O-C). UV–Vis (DMF) λ_{max}/nm (log ε): 365 (4.76), 694 (5.18).

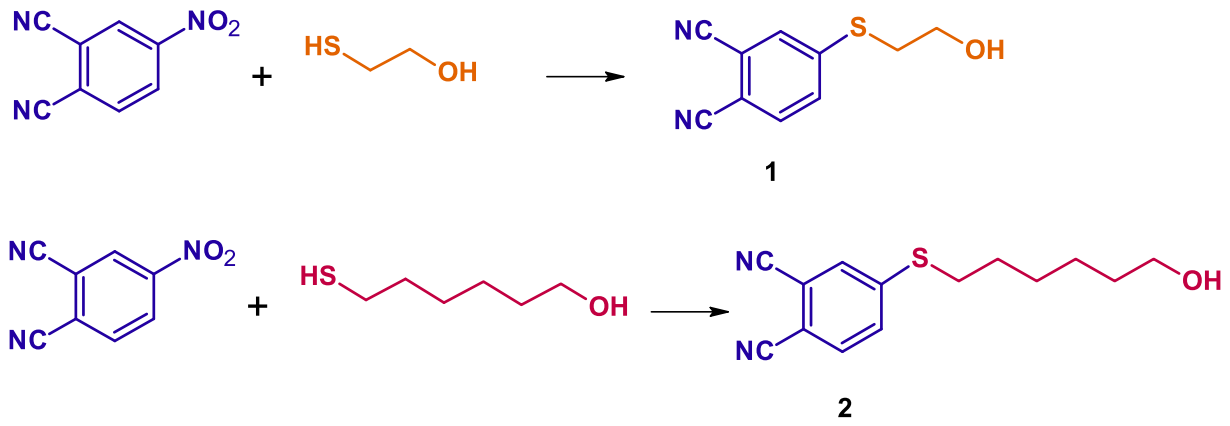
Compound ***8b:*** Yield: 65 mg (%75). ^{1}H NMR (500 MHz, DMSO-d_6) δ 7.42–7.39 (m, Ar—H, 8H), 7.30–7.25 (m, Ar—H, 4H), 3.67–3.62 (m, CH_2, 32H), 3.54–3.46 (m, CH_3, 72H), 2.66–2.64 (m, CH_2, 16H), 1.93–1.88 (m, CH_2, 16H). FT-IR ν (cm^{-1}): 3055 (aromatic C—H), 2929–2856 (aliphatic C—H), 1397 (C—N), 1051 (C-O-C). UV–Vis (DMF) λ_{max}/nm (log ε): 362 (5.16), 702 (5.65).

3. Results and discussion

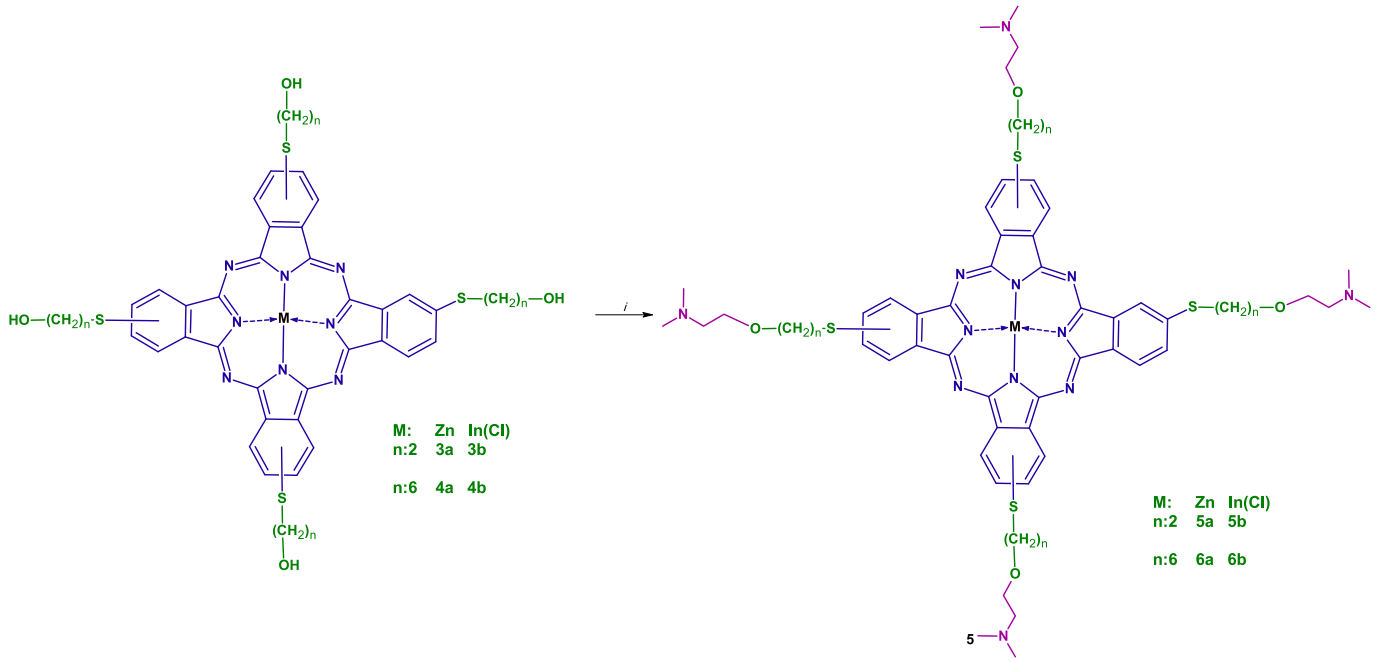
3.1. Synthesis and characterization

In this study, the synthesis of tetra-substituted zinc and indium phthalocyanines containing two different aliphatic groups was aimed. In the first stage, 4-(2-hydroxyethylsulfanyl) phthalonitrile and 4-(6-hydroxyhexylsulfanyl)-1,2-dicyanobenzene were synthesized according to methods reported in the literature (Scheme 1). Zinc and indium phthalocyanine derivatives were then synthesized by reacting dinitrile derivatives with metal salts (Schemes 2 and 3). Subsequently, these phthalocyanine derivatives were reacted with 2-chloro-*N*,*N*-dimethylethylamine hydrochloride in the presence of sodium hydride to obtain the target phthalocyanine derivatives. All synthesized compounds were fully characterized, and the results are in agreement with the proposed structures.

In the FT-IR spectra of compounds **3b** and **4b**, aromatic and aliphatic CH vibrations were marked about 3065–3045 and 2928–2870 cm^{-1}, respectively. In the MALDI-TOF spectrum of **3b**, the peak belonging to the $[M\text{-}Cl]^+$ ion was observed at 929.32. In the ^{1}H NMR spectrum of **3b**, aliphatic protons are seen at 4.22 and 2.30 ppm, while the OH proton was observed at 5.20 ppm. The aromatic protons appeared at 8.39 and 7.94 ppm. The peak belonging to $[M\text{-}Cl]^+$ ion was observed at 1155.30 in the MALDI-TOF spectrum of **4b**. In the ^{1}H NMR spectrum of **4b**, CH_2 protons were observed at 3.55–3.53, 3.00–2.94, 2.66–2.64, and 1.93–1.88 ppm, while the proton of the OH group was detected at 4.36–4.35 ppm. The aromatic protons are found at 7.71–7.54 ppm.



Scheme 1. Synthesis of dinitrile derivatives.



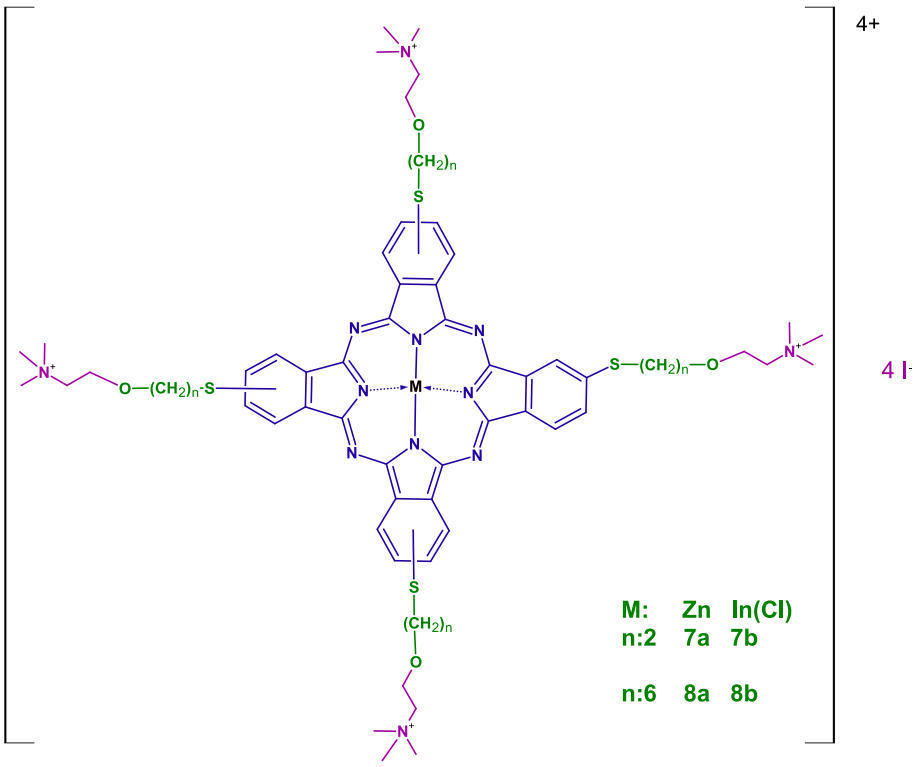
Scheme 2. Synthesis of the phthalocyanines (i) 2-chloro-*N*,*N*-dimethylethylamine hydrochloride, sodium hydride and toluene, 50 °C, 24 h.

Macrocyclic phthalocyanine systems are characterized by Soret and Q bands. Both are fairly strong absorption bands in the UV region, with the Soret band appearing at 300–350 nm and the Q band appearing at 600–700 nm in the visible region. Both bands are associated with $\pi \rightarrow \pi^*$ transitions [34,35]. In the UV–Vis spectra of compounds **3b** and **4b**, the B bands were observed around 380 nm, while the Q bands were observed at 709 and 723 nm, respectively.

In the FT-IR spectra of **5a** and **5b** compounds, aliphatic and aromatic CH vibrations were observed between 3060 and 3050 and 2920–2873 cm^{-1}. While the peaks belonging to CH_3 group in the ^1H NMR spectrum of **5a** compound were observed at 2.18–2.13 ppm, aliphatic CH_2 protons appeared at 4.15 and 1.18–1.19 ppm. The aromatic protons are observed at 7.10–7.15 and 7.55–7.61 ppm. In the proton NMR spectrum of **5b**, the peaks belonging to CH_3 and CH_2 groups were observed at 4.41, 4.12–4.07, and 1.91–1.89 ppm. Peaks belonging to the aromatic ring were detected at 8.39 and 7.94 ppm. In the mass spectra of compounds (**5a** and **5b**), molecular ion peaks were obtained at 1165.47 $[M]^+$ and 1251.85 $[M]^+$, respectively. In the UV–Vis spectra of **5a** and **5b** recorded in DMSO, the B band was observed at 365 and 342 nm, and the Q band was observed at 693 and 687 nm.

In the FT-IR spectra of **6a** and **6b** compounds, aliphatic and aromatic CH vibrations were observed between 3050 and 3031 and 2928–2857 cm^{-1}. While the peaks belonging to the CH_3 group were observed at 1.21 ppm in the ^1H NMR spectrum of **6a** compound, the peaks of CH_2 protons were observed at 1.43–1.46, 1.54–1.61, 1.86–1.88, and 3.40–3.46 ppm. The aromatic protons were detected at 8.07–8.09 and 9.17–9.24 ppm. In the proton NMR spectrum of **6b**, peaks belonging to CH_3 and CH_2 groups were observed at 2.74–2.73, 2.26–2.18, 2.14–1.88, and 0.84–0.74 ppm. Peaks belonging to the aromatic ring were detected at 8.47 and 7.31–7.16 ppm. In the mass spectra of compounds **6a** and **6b**, molecular ion peaks were obtained at 1347.30 $[M\text{-}(CH_3)N]^+$ for compound **6a**, and 1436.46 $[M\text{-}Cl]^+$ for compound **6b**. In the UV–Vis spectra of **6a** and **6b**, the Q band was observed at 695 and 689 nm while the B band was observed at 364 and 350 nm, respectively.

The FT-IR spectra of compounds **7a**, **7b**, **8a** and **8b** are in good agreement with the proposed structures. While CH_3 protons were observed at 2.54 ppm in the ^1H NMR spectrum of the **7a** compound, the peaks belonging to CH_2 protons were observed at 5.01 and 3.66–3.09 ppm. 8 aromatic protons at 8.85–8.78 ppm and 4 aromatic protons at 8.10–8.00 ppm were observed. In the proton NMR spectrum of **7b**, the peaks belonging to CH_3 and CH_2 groups were observed at 2.73–2.68, 1.92–1.87, and 1.39–1.36 ppm. The aromatic protons were detected at



Scheme 3. Chemical structures of the target tetra-substituted quaternized phthalocyanine derivatives containing aliphatic chains.

7.69–7.59 ppm. In the ^{1}H NMR spectrum of **8a** compound, peaks belonging to CH_3 group were observed at 3.18–3.17 ppm, while CH_2 protons were observed at 3.51–3.48, 1.22, and 0.84 ppm. The aromatic protons were detected at 9.18 and 8.48 ppm. In the proton NMR spectrum of **8b**, CH_3 and CH_2 protons were observed at 3.67–3.62, 3.54–3.46, 2.66–2.64, and 1.93–1.88 ppm. Peaks belonging to the aromatic ring were detected at 7.42–7.39 and 7.30–7.25 ppm. The UV–vis spectrum of **7a** and **8a** in DMSO exhibited a typical B band around 360–370 nm and a Q band at 678 and 692 nm, respectively. The B bands of **7b** and **8b** compounds were observed around 370–380 nm, while the Q bands were observed at 704 and 702 nm, respectively.

3.2. *Fluorescence quantum yields of the synthesized phthalocyanine derivatives*

The fluorescence quantum yields (Φ_F) of the synthesized phthalocyanine derivatives were determined in DMSO using unsubstituted ZnPc as the standard. To determine the photophysical properties of the synthesized phthalocyanine derivatives, their fluorescence quantum yields (Φ_F) were measured, and the resulting data are presented in Table 1. The calculated yields were found to be lower than those of the standard unsubstituted zinc phthalocyanine. This decrease is attributed to the presence of electron-donating alkyl groups on the phthalocyanine ring, which promotes the transition from the excited singlet state to the triplet state via intersystem crossing (ISC), thereby reducing the fluorescence efficiency. Upon comparing the results, it was determined that the fluorescence quantum yields increased in correlation with the length of the aliphatic chains. Long aliphatic chains enhance the solubility of the molecules in organic solvents, allowing for better dispersion. This increased solubility reduces aggregation-induced quenching, thereby indirectly supporting a higher fluorescence yield.

Quaternized phthalocyanines exhibited higher fluorescence quantum yields compared to their non-quaternized analogs. The quaternization of phthalocyanines via peripheral groups enhances the fluorescence quantum yield by electrostatically inhibiting intermolecular aggregation. This modification preserves the monomeric form of the macrocycles in solution, thereby preventing non-radiative relaxation pathways associated with aggregate formation. Upon comparing indium and zinc phthalocyanines, it was observed that the indium derivatives exhibited lower fluorescence quantum yields. This finding is consistent with the existing literature and is attributed to the heavy atom effect of the indium metal. Due to its high atomic number, indium induces a pronounced “internal heavy atom effect,” which enhances spin-orbit interaction (SOI). This increased interaction facilitates a rapid transition from the excited singlet state to the triplet state through intersystem crossing (ISC). Consequently, the radiative decay pathway (fluorescence) is suppressed in favor of non-radiative triplet state formation.

The natural radiative lifetime (τ_0 or τ_{rad}) represents the theoretical duration a molecule would remain in the excited state if its return to the

Table 1
Fluorescence quantum yields of the synthesized phthalocyanine derivatives.

	Φ_F[a,b]	τ_0 (ns)	τ_F (ns)
ZnPc(standard)	0,17		3.1
3a	0.0734	8.83	0.65
5a	0.1060	7.90	0.84
7a	0.1473	2.86	0.42
4a	0.1336	6.31	0.84
6a	0.1404	5.36	0.75
8a	0.1533	4.84	0.74
3b	0.0527	3.51	0.19
5b	0.0677	3.50	0.24
7b	0.0793	3.54	0.28
4b	0.0416	1.72	0.07
6b	0.0649	1.33	0.09
8b	0.0827	2.74	0.23

[a] The natural radiative lifetimes (τ_0) were calculated from the experimental absorption and fluorescence spectra using the Strickler-Berg equation [36].
[b] Fluorescence quantum yields (Φ_F) were determined relative to unsubstituted ZnPc in DMSO with an estimated experimental uncertainty of ±5%.

ground state occurred exclusively through the emission of light (fluorescence). Essentially, it defines the excited state's duration in the absence of all non-radiative decay pathways, such as vibrational relaxation (heat loss) or intersystem crossing to the triplet state. Fluorescence lifetime (τ_F) represents the average duration a molecule remains in the excited singlet state (S_1) before returning to the ground state (S_0). Essentially, this parameter serves as a measure of the rate at which the excited molecule interacts with various deactivating channels. The incorporation of aliphatic (alkyl) chains into the phthalocyanine framework, as well as the length of these chains, modulates the fluorescence lifetime (τ_F) through both direct electronic effects and intermolecular interactions, such as aggregation. The results obtained from these measurements are presented in Table 1.

3.3. Singlet oxygen quantum yields of the quaternized phthalocyanines

Within the scope of the study, the singlet oxygen quantum yields (Φ_Δ) of the metallophthalocyanines were calculated. Unsubstituted zinc phthalocyanine was used as a standard. The results are satisfactory for the potential use of the synthesized phthalocyanines in Photodynamic Therapy (PDT), as shown in Table 2. When compared with the singlet oxygen quantum yield of the standard zinc phthalocyanine, it was determined that the synthesized zinc and indium phthalocyanine derivatives exhibited higher quantum yields. Furthermore, the zinc phthalocyanine derivatives exhibited higher yields than the indium phthalocyanine derivatives due to the metal effect. Although heavier central metal ions such as indium (III) typically enhance spin-orbit coupling and promote intersystem crossing (ISC), the lower singlet oxygen quantum yields observed for the indium derivatives compared to their zinc analogues can be rationalized by competitive deactivation pathways and structural factors. Specifically, In (III) phthalocyanines are frequently more prone to aggregation in solution due to axial coordination, which acts as a major non-radiative relaxation channel and quenches the triplet state. Furthermore, structural distortions induced by axial ligands and the fine-tuning of the singlet-triplet energy gap can alter the efficiency of triplet state population. Similar trends where Zn (II) phthalocyanines outperform heavier metal counterparts in singlet oxygen generation have been reported previously in the literature [37–39].

3.4. Antioxidant activity of phthalocyanines

Antioxidant compounds provide the removal and prevention of free radicals resulting from some metabolic reactions of the living organism and external factors. Some of the vitamins are natural antioxidants. Due to the inadequacy and rapid degradation of natural antioxidants, synthetic antioxidants such as BHT and BHA are widely used in the pharmaceutical and food industries [40]. The rapid increase in population and technology in recent years has led to increased research on newly synthetic antioxidants. For this purpose, the antioxidant properties of phthalocyanines have also begun to be investigated [41–44]. In this study, the antioxidant properties of the phthalocyanine derivatives were investigated. The DPPH assay was used to estimate the cell-free radical-scavenging activity of the phthalocyanine derivatives. In this assay, reduction of the DPPH radical by electron- or hydrogen-donating molecules results in a decrease in absorbance at 517 nm, accompanied by a colour change from purple to yellow.

The free radical scavenging activities of phthalocyanine compounds were determined quantitatively using DPPH. Fig. 1 shows the results of this test. The radical scavenging activity of phthalocyanines was compared to that of BHT as a standard at the same dose, and the percent inhibition against DPPH was calculated. At 1000 μg/mL, BHT exhibited 88.0% radical-scavenging activity, whereas the phthalocyanine derivatives showed activities ranging from 4.0% to 53.8%. (Fig. 1). For **7b**, RSA was detectable only for 125 μg/mL. When the results were examined, it was determined that compound **5b** had the highest radical scavenging activity with 53.8%. The order of DPPH radical scavenging activity of the synthesized complexes is as follows: **5b** > **8b** > **5a** > **6a** > **7a** > **8a** > **6b** > **7b**.

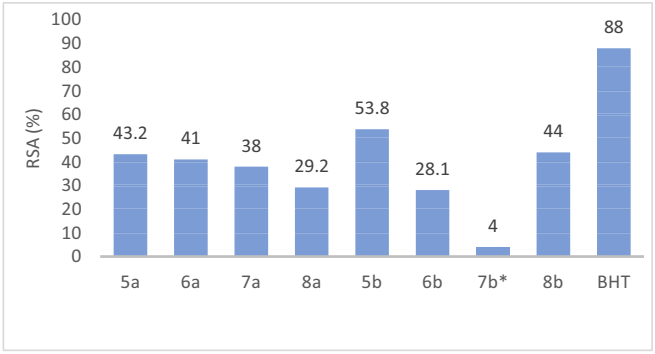


Fig. 1. Radical scavenging activity (%) of the phthalocyanine derivatives at a concentration of 1000 μg/mL. *For 7b, RSA was detectable only for 125 μg/mL.

Previous studies have also reported DPPH radical-scavenging activity for structurally different phthalocyanine derivatives. Cobalt phthalocyanine–gold nanoparticle conjugates were reported to exhibit antioxidant activity [22]. Atilla et al. reported maximum DPPH inhibition values of 40.46% and 25.76% for ZnPc and MgPc, respectively, at 100 mg L^{-1} [45]. Similarly, zinc and indium phthalocyanines bearing (E)-4-(4-((thiophen-2-ylmethylene)amino)phenoxy) substituents exhibited DPPH radical-scavenging activity [46]. In the present study, the derivatives showed radical-scavenging activities ranging from 4.0% to 53.8% at 1000 μg/mL, with compound **5b** exhibiting the highest activity. However, direct comparison of antioxidant potency among these studies should be made cautiously because of differences in compound structures, assay concentrations, and experimental conditions. Moreover, the activity ranking observed in the present study did not indicate a consistent monotonic relationship with chain length or metal centre.

Phthalocyanines are prone to solvent- and concentration-dependent aggregation, which may influence their apparent radical-scavenging activity [42]. Therefore, the differences observed in the DPPH assay may reflect not only intrinsic electron- or hydrogen-donating capacity but also differences in aggregation state, solubility, and accessibility of reactive sites under the assay conditions. Because concentration-dependent UV–Vis measurements were not performed under the specific DPPH assay conditions, the aggregation state of the derivatives could not be established. Accordingly, the present results should be interpreted as apparent radical-scavenging activities under the tested conditions, and no definitive aggregation- or chain-length-dependent antioxidant mechanism is claimed.

3.5. Cell culture

Cells were successfully cultured throughout the cell culture study, with no signs of contamination observed before or after incubation with the synthesized samples. Although no marked morphological alterations were observed under the specified experimental conditions, cellular morphology was not considered a direct indicator of cell viability. Therefore, cell viability was evaluated quantitatively using the MTT assay.

Table 2
Singlet oxygen quantum yields of the quaternized phthalocyanine derivatives.

Compound	Φ_Δ	Compound	Φ_Δ
7a	0.67	**7b**	0.61
8a	0.68	**8b**	0.56

3.6. Incubation of cells with synthesized metalated-phthalocyanines

As a result of incubation of cells with metallophthalocyanines, morphologic changes were observed in the cells. The shape of the cells incubated with the compounds changed, and membrane integrity was affected.

3.7. MTT (3-(4,5-dimethylthiazol-2-yl)-2,5-diphenyltetrazolium bromide) anticancer/cytotoxicity tests

In the MTT test performed after incubation of the cells with the synthesized samples, it was determined that the IC50 value of the dark and light groups was almost the same concentration between the groups. According to this result, it was determined that the samples were not more active with this light applied. IC_{50} values of the samples are given in Table 3.

The cytotoxic activity of the synthesized compounds differed between the two colorectal cancer cell lines. Compound **7a** exhibited the highest activity in HT-29 cells based on its IC_{50} value of 50 μg/mL. However, its IC_{50} value in DLD-1 cells was 750 μg/mL, indicating substantially lower activity in this cell line. Therefore, compound Although phthalocyanines may exhibit phototoxic **7a** cannot be considered the most effective compound overall; rather, it demonstrated the highest activity specifically against HT-29 cells. In DLD-1 cells, compounds **5b** and **6b** were the most active compounds, each exhibiting an IC_{50} value of 125 μg/m. These findings demonstrate that the relative activity of the synthesized compounds was dependent on the cell line examined. The MTT-derived cell viability results are presented in Figure 2, 3, 4 and 5.

According to the results, the compounds generally caused a concentration-related reduction in MTT-derived cell viability in DLD-1 cells. At the highest tested concentration of 1000 μg/mL, all compounds produced marked antiproliferative effects. With the exception of compound 5a, the effects of the tested compounds at this concentration were greater than those of cisplatin, which was used as the positive control. Compounds **6a**, **7a**, **8a**, **5b**, **6b**, **7b**, and **8b** produced comparable reductions in MTT-derived cell viability at the highest concentration. In contrast to their effects at higher concentrations, compounds **7a** and **8a** produced MTT signals above the control level at the lower concentrations of 62.5 and 125 μg/mL. This observation indicates a non-monotonic concentration–response pattern. However, because the MTT assay measures cellular metabolic activity and does not directly quantify cell proliferation, the increased MTT signal at these concentrations cannot conclusively be interpreted as enhanced cell proliferation.

Most compounds produced an overall concentration-related reduction in MTT-derived HT-29 cell proliferation. However, compound **6a** exhibited a more complex, non-monotonic concentration–response pattern. At the lower concentrations of 62.5 and 125 μg/mL, the MTT signal was higher than in the control group, whereas higher concentrations exhibited an antiproliferative effect. Therefore, the activity of compound **6a** should not be described as a simple dose-dependent antiproliferative response. Moreover, because an increased MTT signal may reflect altered cellular metabolic activity rather than an actual increase in cell number, further proliferation-specific assays would be required to determine the biological basis of this low-concentration response.

Pronounced differences in sensitivity between DLD-1 and HT-29 cells were observed for some compounds, particularly **7a**, **8a**, and **7b**. These differences indicate that structurally related phthalocyanine derivatives may elicit distinct biological responses across colorectal cancer cell lines. Such cell-line-dependent responses could potentially be associated with differences in cellular uptake, intracellular accumulation, metabolic activity, drug-efflux mechanisms, or susceptibility to cell-death signalling. However, these mechanisms were not examined in the present study. Further studies are therefore required to determine the molecular basis of the differential sensitivity of DLD-1 and HT-29 cells.

The results indicated that among the zinc phthalocyanine derivatives, **5a** exhibited the highest activity in DLD-1 cells ($IC_{50} = 200$ μg/mL), whereas **7a** exhibited the highest activity in HT-29 cells ($IC_{50} = 50$ μg/mL). Within the indium phthalocyanine series, **5b and 6b** exhibited the highest activity in DLD-1 cells, with IC_{50} values of 125 μg/mL**,** whereas **8b** showed the highest IC_{50} value in HT-29 cells (250 μg/mL)**.** Given that no statistically significant differences in cytotoxic activity were observed between the dark and light-exposed groups, no significant light-induced enhancement of cytotoxicity was observed under the experimental conditions employed in this study. Consequently, these compounds did not exhibit a detectable light-induced enhancement of cytotoxicity under the irradiation conditions employed in this study.

In a 2022 study, the MTT test of the synthesized asymmetric phthalocyanine compound was performed. It was found that although it showed high phototoxicity against TNBC cells, its cytotoxicity was low. Therefore, it was determined to be applied to healthy cells without giving harm to them [46,47]. Huang et al. studied the photodynamic activities of axial morpholine-substituted silicon phthalocyanine against B16 melanoma cells. The compound was not cytotoxic in the absence of light but exhibited high photocytotoxicity after exposure to red light. IC50 values, defined as the concentration of photosensitizer required to kill 50% of the cells, were approximately 0.30 μM [48]. In a 2017 study by Qui et al., the conjugate of silicon (IV) phthalocyanine with biotin was studied for tumor-targeted photodynamic therapy. Without irradiation by MTT assay, silicon complexes were found to have almost no toxicity to HeLa cells at concentrations ranging from 10 μM to 4 μM. Cells showed high cytotoxicity of phthalocyanine derivatives in the presence of red light ($\lambda \approx 670$ nm). IC_{50} values for the compounds were obtained between 0.04 and 0.46 μM [49]. Compared to the literature, the phthalocyanines can be suitable materials for photodynamic applications after further investigation.

Table 3
The IC_{50} value of the samples, in μg/mL.

Compound	DLD-1		HT-29		cLogP
	Dark incubation	Light-exposed group	Dark incubation	Light-exposed group	
5a	200 ± 14	200 ± 13	250 ± 13	250 ± 12	4.05
6a	650 ± 28	650 ± 22	300 ± 15	300 ± 19	9.83
7a	750 ± 36	750 ± 23	50 ± 8	50 ± 8	−3.50
8a	500 ± 27	500 ± 16	100 ± 11	100 ± 7	6.00
5b	125 ± 9	125 ± 8	100 ± 5	100 ± 7	4.65
6b	125 ± 10	125 ± 8	100 ± 4	100 ± 6	10.81
7b	200 ± 11	200 ± 11	750 ± 19	750 ± 18	−2.90
8b	300 ± 13	300 ± 12	250 ± 8	250 ± 11	6.53

3.8. Structure–activity relationship (SAR) and computational lipophilicity analysis

To gain deeper mechanistic insights into the in vitro anticancer profiles of the synthesized phthalocyanines, theoretical lipophilicity values (cLogP) were calculated via SwissADME and correlated directly with the experimental IC_{50} data (Table 3). These calculated parameters quantitatively confirm the anticipated hydrophobic enhancement driven by the elongation of peripheral alkyl chains, moving from moderate values of 4.05–4.65 in short-chain neutral complexes to significantly higher levels of 9.83–10.81 in their long-chain counterparts. Conversely, the quaternization substantially altered the predicted lipophilicity, with cLogP values ranging from −3.50 to 6.53, depending on the metal center and peripheral structure.

When evaluating these findings alongside the in vitro cytotoxicity results across the DLD-1 and HT-29 cancer cell lines (Table 3), several compelling structure-activity trends emerge. First, the identical IC_{50} metrics recorded across both dark incubation and light-exposed environments strongly point toward a light-independent cytotoxic mechanism under these experimental conditions, ruling out a classical

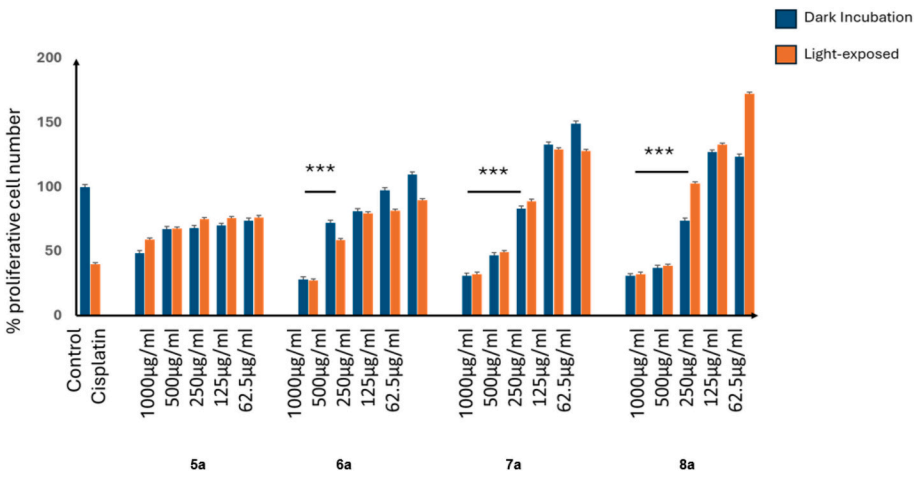


Fig. 2. DLD1% cell proliferation with compounds **5-8a**.

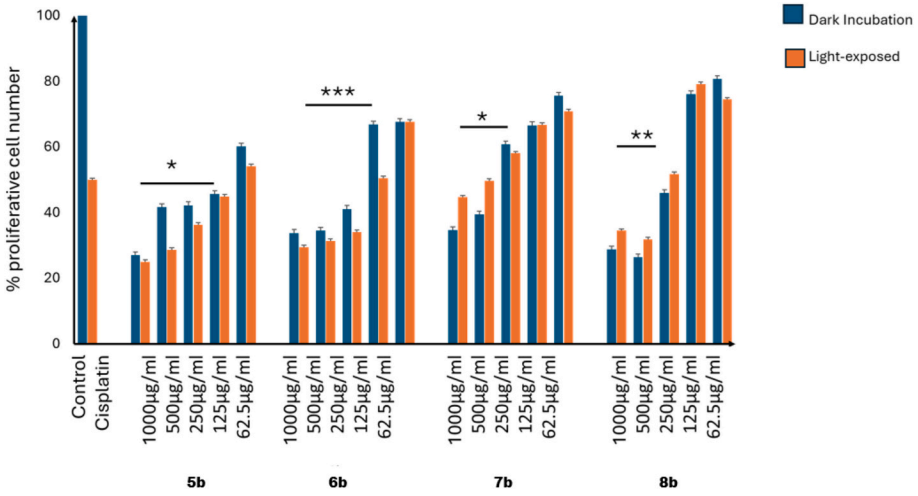


Fig. 3. DLD1% cell proliferation with compounds **5-8b**.

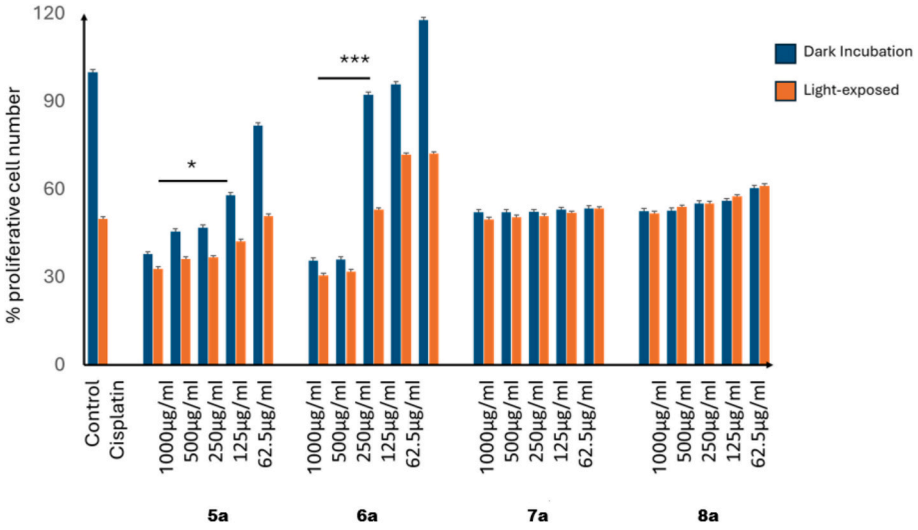


Fig. 4. HT29% cell proliferation with compounds **5-8a**.

photodynamic therapeutic (PDT) response. Furthermore, distinct derivatives—most notably compound **7a**—display pronounced cell-line selectivity, showing a remarkable IC_{50} of 50 µg/mL against HT-29 cells while remaining far less active against the DLD-1 line. Taken together, these insights demonstrate that biological efficacy relies heavily on striking an optimal balance between lipophilic membrane affinity and

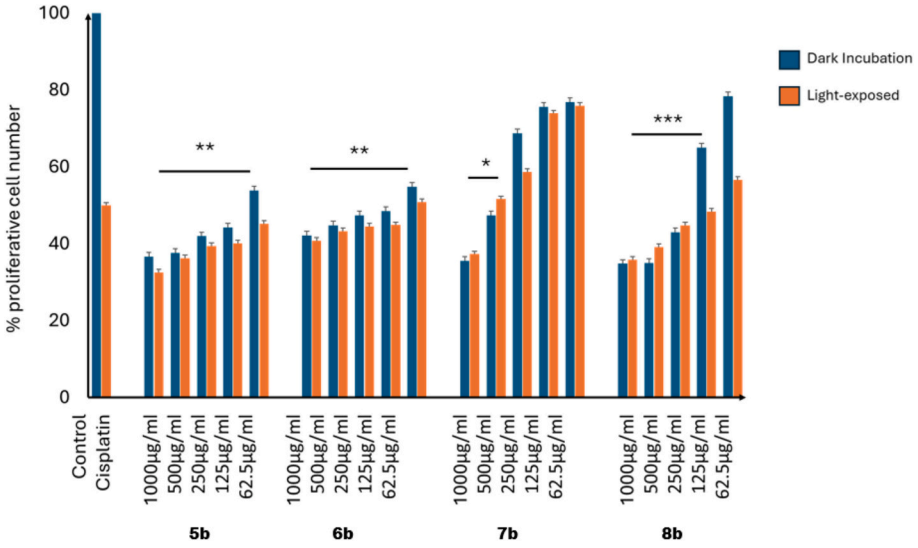


Fig. 5. HT29% cell proliferation with compounds **5-8b**.

sufficient aqueous solubility.

The structure-activity relationship (SAR) observed between alkyl chain length, quaternary substitution, and anticancer activity underscores just how critical physicochemical properties are in dictating cellular behavior. Although extending the alkyl chains significantly increases lipophilicity—pushing cLogP values up to 10.81 for compound **6b**— may increase the tendency for aggregation in aqueous media and consequently reduce the fraction of freely available monomeric species. In contrast, the quaternary derivatives, particularly compound **7a**, adopt a hydrophilic character (cLogP of −3.50) that guarantees exceptional dispersion in the extracellular milieu.

While classical passive transmembrane diffusion is typically favored within intermediate lipophilicity windows, the high cytotoxicity of compound **7a** against the HT-29 cell line (IC_{50}: 50 µg/mL) suggests that alternative mechanisms govern its cellular internalization. These findings may indicate that cellular uptake of **7a** is not governed solely by passive diffusion and could involve electrostatic membrane interactions and/or endocytic processes.Moreover, the clear selectivity observed between the DLD-1 and HT-29 lines highlights how structural modifications—such as the selection of the central metal (Zn vs. In) and peripheral substituents—finely tune target engagement and membrane affinity, successfully elevating the SAR from a purely descriptive observation into a mechanistically driven framework.

3.9. Comparison of cytotoxic activity with cisplatin

Given that the dark and light-exposed IC_{50} values were nearly identical, no significant light-induced enhancement of cytotoxicity was observed under the experimental conditions used in this study. Therefore, the synthesized compounds were further evaluated under dark conditions and compared with Cisplatin [50].

In DLD-1 cells, compounds **5b** and **6b** showed the highest activity among the indium phthalocyanine derivatives, with IC_{50} values of 125 µg/mL. However, Cisplatin showed a substantially lower reported IC_{50} value (~11.4 µg/mL) in DLD-1 cells, indicating higher cytotoxic potency under the reported conditions [50]. In contrast, compound **7a** showed the highest activity among the synthesized compounds in HT-29 cells, with an IC_{50} value of 50 µg/mL. Although this result indicates notable activity against HT-29 cells, the present data are insufficient to conclude that **7a** overcomes platinum-resistance mechanisms.

Overall, the synthesized phthalocyanine derivatives cannot be considered more cytotoxic than Cisplatin based solely on the IC_{50} values. Nevertheless, their cytotoxic activity in the absence of light, particularly that of **7a** in HT-29 cells, makes them promising candidates for further investigation.

3.10. Testing cell apoptosis with annexin V

After incubation of the cells with the synthesized compounds, the cells were tested with Annexin V for apoptosis. With this test, healthy living cells, dead cells, and early apoptotic and late apoptotic cells were determined. The test was performed using flow cytometry with 1000 event counts. The results are presented in Table 4. According to the results, the compounds have apoptotic effects on the cells. The highest amount of apoptosis was observed in DLD1 cells with compound **8b**, whereas in HT29 cells with compound **7b**. It is seen that the late apoptosis rate of the compounds in the cells is statistically significantly higher than the early apoptosis rate. The Annexin V flow-cytometry profiles showed treatment-associated changes in the distribution of viable and apoptosis-associated cell populations in both DLD-1 and HT-29 cells. Several compounds produced a shift from the viable quadrant toward the early- and/or late-apoptotic quadrants compared with the

Table 4
Apoptosis test results of the samples.

Compound	DLD-1			
	Living cell	Dead cell	Early apoptosis	Late apoptosis
Control	65.8	30.2	1.72	2.21
5a	18.6	0.5	0	80.9
6a	72.1	9.3	0	18.6
7a	80	0	0	20
8a	61.5	23.1	7.69	7.69
5b	0	0	0	100
6b	0	0	13.7	86.3
7b	12	0	16	72
8b	2.07	0.21	0	97.7
	HT29			
	Living cell	Dead cell	Early apoptosis	Late apoptosis
Control	70.3	12.8	1.08	15.7
5a	13.5	15.7	0	70.9
6a	24.9	18.6	0.55	55.9
7a	55.3	17.5	2.91	24.3
8a	33.8	17.6	2.7	45.9
5b	23.2	24.2	0	52.5
6b	27.3	32.8	0	39.9
7b	3.7	9.4	0	86.9
8b	66.9	13.4	0	19.7

corresponding control. These findings were consistent with the changes in cell viability observed in the MTT assay and further supported the apoptotic involvement in the cytotoxic response of the synthesized derivatives.

The results of the study indicated that the indium phthalocyanine series induced substantial apoptotic effects in DLD-1 and HT29 cells. The observed responses suggest that DLD-1 cells may be particularly sensitive to the indium phthalocyanine derivatives under the experimental conditions employed. The predominance of late-stage apoptosis further supports the ability of these compounds to induce cell death through apoptotic pathways. In particular, compounds **5b**, **6b**, and **7b** showed pronounced apoptotic responses, highlighting their potential for further investigation as anticancer candidates against colorectal cancer. It is recommended that these compounds be studied in detail in in vivo models and at the mechanistic level in the future.

4. Conclusion

This work focuses on the synthesis, chemical characterization, and preliminary cell screening of the new compounds. Tetrasubstituted zinc and indium phthalocyanines with different chain lengths were synthesized. The structures of the synthesized compounds were elucidated by characterization using spectroscopic methods such as ^{1}H NMR, FT-IR, UV–Vis, MALDI-TOF mass spectroscopy. Although the fluorescence quantum yields of quaternized phthalocyanine derivatives are lower than those of the standard unsubstituted zinc phthalocyanine, they represent a compelling alternative due to their excellent aqueous solubility. The free radical scavenging activities of phthalocyanine compounds were determined quantitatively using DPPH. Among the tested derivatives, **5b** exhibited the highest DPPH radical-scavenging activity, followed by **8b** and **5a**; nevertheless, all derivatives were less active than BHT under the tested conditions. These findings indicate compound-dependent radical-scavenging activity but do not establish a definitive relationship with chain length, metal centre, or cellular antioxidant effects. It was examined in vitro cytotoxic and apoptotic effects of the synthesized compounds on DLD-1 and HT-29 colorectal cancer cell lines by MTT and Annexin V assays. The results have shown that these synthesized compounds have cytotoxic and apoptotic effects on these colorectal cell lines. Although phthalocyanines may exhibit phototoxic effects in vitro, no statistically significant difference was found between the dark and white-light groups under the specific irradiation conditions employed in this study. This finding does not exclude the possibility that these compounds may exhibit photosensitivity under different irradiation wavelengths, intensities, or exposure durations, which should be investigated in future studies. Cell tests show that our compounds have a powerful effect on cells when compared to Cisplatin. Some of the compounds have antiproliferative and proliferative effects on cells in a dose-dependent manner. They, however, all affect cell proliferation at high doses. The results show that the compounds are promising in cancer treatment.

CRediT authorship contribution statement

Dilek Bahar: Writing – original draft, Methodology, Investigation. **H. Yasemin Yenilmez:** Writing – original draft, Supervision, Project administration, Conceptualization. **Muazzez Derya-Andeden:** Methodology, Investigation. **Pınar Altin-Celik:** Methodology, Investigation. **Nilgün Güler:** Methodology, Investigation.

Declaration of competing interest

The authors declare that they have no known competing financial interests or personal relationships that could have appeared to influence the work reported in this paper.

Acknowledgments

This study was supported by the Scientific and Technological Research Council of Turkey (TUBITAK) under the Grant Number 123Z124. The authors thank TUBITAK for their support. Hacer Yasemin Yenilmez appreciates the funding from the Research Fund of the Istanbul Technical University (Project Number: TAB- 2024-46360).

Appendix A. Supplementary data

Supplementary data to this article can be found online at https://doi.org/10.1016/j.poly.2026.118433.

Data availability

All data obtained are presented in the supplementary document.

References

[1] N.B. McKeown, Phthalocyanine Materials: Synthesis, Structure, and Function, Cambridge University Press, Cambridge, 1998.
[2] C.C. Leznoff, A.B.P. Lever, Phthalocyanines: Properties and Application, VCHPublishers, New York, 1989.
[3] S. Huang, K. Chen, T.-T. Li, Porphyrin and phthalocyanine based covalent organic frameworks for electrocatalysis, Coord. Chem. Rev. 464 (2022) 214563, https://doi.org/10.1016/j.ccr.2022.214563.
[4] J. Bonelli, E. Ortega-Forte, G. Vigueras, J. Follana-Berná, P. Ashoo, D. Abad-Montero, N. Isidro, M. López-Corrales, A. Hernández, J. Ortiz, E. Izquierdo-García, M. Bosch, J. Rocas, Á. Sastre-Santos, J. Ruiz, V. Marchán, A nanoencapsulated Ir (III)-phthalocyanine conjugate as a promising photodynamic therapy anticancer agent, ACS Appl. Mater. Interfaces 30 (2024) 38916–38930, https://doi.org/10.1021/acsami.4c05181.
[5] E. Demir, H. Silah, B. Uslu, Phthalocyanine modified electrodes in electrochemical analysis, Crit. Rev. Anal. Chem. 52 (2020) 425–461, https://doi.org/10.1080/10408347.2020.1806702.
[6] D. Li, S. Cai, P. Wang, H. Cheng, B. Cheng, Y. Zhang, G. Liu, Innovative design strategies advance biomedical applications of phthalocyanines, Adv. Healthc. Mater. 12 (2023) 2300263, https://doi.org/10.1002/adhm.202300263.
[7] H.Y. Yenilmez, N. Farajzadeh, N. Güler Kuşçulu, D. Bahar, S. Özdemir, G. Tollu, M. Güllü, Z. Altuntaş Bayır, Effect of axial ligand length on biological and anticancer properties of axially disubstituted silicon phthalocyanines, Chem. Biodivers. 20 (2023) e202201167, https://doi.org/10.1002/cbdv.202201167.
[8] D.A. Bunin, A.G. Martynov, D.A. Gvozdev, Y.G. Gorbunova, Phthalocyanine aggregates in the photodynamic therapy: dogmas, controversies, and future prospects, Biophys. Rev. 15 (2023) 983–998, https://doi.org/10.1007/s12551-023-01129-7.
[9] C.C. Rennie, R.M. Edkins, Targeted cancer phototherapy using phthalocyanine–anticancer drug conjugates, Dalton Trans. 51 (2022) 13157–13175, https://doi.org/10.1039/D2DT02040H.
[10] A. Galstyan, Turning photons into drugs: phthalocyanine-based photosensitizers as efficient photoantimicrobials, Chemistry (Weinheim an der Bergstrasse, Germany) 27 (2021) 1903–1920, https://doi.org/10.1002/chem.202002703.
[11] L.A. Cooper, E.G. Demicco, J.H. Saltz, R.T. Powell, A. Rao, A.J. Lazar, PanCancer insights from the Cancer genome atlas: the pathologist's perspective, J. Pathol. 244 (2018) 512–524, https://doi.org/10.1002/path.5028.
[12] R.L. Siegel, K.D. Miller, H. Fuchs, A. Jemal, Cancer statistics, 2021, CA Cancer J. Clin. 71 (2021) 7–33, https://doi.org/10.3322/caac.21654.
[13] A. Esmeeta, S. Adhikary, V. Dharshnaa, P. Swarnamughi, Z.U. Maqsummiya, A. Banerjee, S. Pathak, A.K. Duttaroy, Plant-derived bioactive compounds in colon cancer treatment: an updated review, Biomed. Pharmacother. 153 (2022) 113384, https://doi.org/10.1016/j.biopha.2022.113384.
[14] U. Anand, A. Dey, A.K.S. Chandel, R. Sanyal, A. Mishra, D.K. Pandey, V. De Falco, A. Upadhyay, R. Kandimalla, A. Chaudhary, J.K. Dhanjal, S. Dewanjee, J. Vallamkondu, J.M. Pérez de la Lastra, Cancer chemotherapy and beyond: current status, drug candidates, associated risks and progress in targeted therapeutics, Genes Dis. 10 (2023) 1367–1401, https://doi.org/10.1016/j.gendis.2022.02.007.
[15] W. Wu, Y. Pu, J. Shi, Nanomedicine-enabled chemotherapy-based synergetic cancer treatments, J. Nanobiotechnol. 20 (2022) 4, https://doi.org/10.1186/s12951-021-01181-z.
[16] M. Galanski, M.A. Jakupec, B.K. Keppler, Update of the preclinical situation of anticancer platinum complexes: novel design strategies and innovative analytical approaches, Curr. Med. Chem. 12 (2005) 2075–2094, https://doi.org/10.2174/0929867054637626.
[17] A.M.P. Romani, Cisplatin in cancer treatment, Biochem. Pharmacol. 206 (2022) 115323, https://doi.org/10.1016/j.bcp.2022.115323.
[18] M.S. Rahman (Ed.), Handbook of Food Preservation, CRC Press, New York, US, 2007.
[19] V. Lobo, A. Patil, A. Phatak, N. Chandra, Free radicals, antioxidants and functional foods: impact on human health, Pharmacogn. Rev. 4 (8) (2010) 118–126, https://doi.org/10.4103/0973-7847.70902.

[20] M. Carocho, I.C.F.R. Ferreira, A review on antioxidants, prooxidants and related controversy: natural and synthetic compounds, screening and analysis methodologies and future perspectives, Food Chem. Toxicol. 51 (2013) 15–25, https://doi.org/10.1016/j.fct.2012.09.021.
[21] M.S. Ağırtaş, B. Cabir, Ü. Yıldıko, S. Özdemir, S. Gonca, Synthesis, antioxidant, DNA cleavage and antimicrobial properties of phthalocyanine complexes bearing the poly-hydroxyl groups, Chem. Pap. 75 (2021) 1749–1760, https://doi.org/10.1007/s11696-020-01432-7.
[22] I. Göller, H.Y. Yenilmez, N.F. Öztürk, Biological properties of 4-trifluoromethyl-benzyloxy-substituted cobalt phthalocyanine-gold nanoparticle conjugates, Appl. Organomet. Chem. 38 (2024) e7505, https://doi.org/10.1002/aoc.7505.
[23] F. Çelik, Y. Ünver, F. OzTuncay, U. Cakmak, Y. Kolcuoglu, K.K. Uzun, H. Ozturk, N. Yorulmaz, İ. Değirmencioğlu, Synthesis and characterization of newly phthalocyanine molecules: their enzyme inhibition and antioxidant properties, in silico and in vitro, J. Organomet. Chem. 1016 (2024) 123237, https://doi.org/10.1016/j.jorganchem.2024.123237.
[24] B. Çuhadar, A.K. Burat, G. Giray, S. Özdemir, Non-peripheral and peripheral tetrasubstituted metallophthalocyanines having dichlorophenylthio groups as novel biological active materials for antioxidant, DNA cleavage, antimicrobial, and biofilm inhibition activities, Polyhedron 244 (2023) 116593, https://doi.org/10.1016/j.poly.2023.116593.
[25] Ö. Sağlam, M. Akin, H.P. Karaoğlu, N. Saki, M.B. Koçak, Investigation of time-kill evaluation and antioxidant activities of new tetra-substituted metallophthalocyanines bearing 4-(trifluoromethoxy)thiophenyl groups, ChemistrySelect 5 (2020) 2522–2527, https://doi.org/10.1002/slct.201904636.
[26] K. Kanagaraj, S. Nangan, N. Thirumalaivasan, Carbon dots and their role in cancer immunotherapy: targeted drug delivery and tumor microenvironment modulation-a narrative review, Next Mater. 11 (2026) 101711, https://doi.org/10.1016/j.nxmate.2026.101711.
[27] N. Thirumalaivasan, K. Kanagaraj, S. Nangan, R. Pothu, S.P. Rajendra, P. Karuppiah, R. Boddula, Bioactive hydrogels (bio-HyGs): emerging trends in drug delivery and wound healing applications, Polym. Adv. Technol. 36 (4) (2025) e70132, https://doi.org/10.1002/pat.70132.
[28] N. Thirumalaivasan, S. Nangan, D. Verma, M. Shellaiah, S. Ali, S. Rajendran, K. Kanagaraj, R. Pothu, R. Boddula, A.B. Radwan, N. Al-Qahtani, Exploring the diverse nanomaterials employed in dental prosthesis and implant techniques: an overview, Nanotechnol. Rev. 14 (1) (2025) 20250140, https://doi.org/10.1515/ntrev-2025-0140.
[29] S. Gürsoy, A. Cihan, M.B. Koçak, Ö. Bekaroğlu, Synthesis of new metal-free and metal-containing phthalocyanines with tertiary or quaternary aminoethyl substituents, Monatsh. Chem. 132 (2001) 813–819, https://doi.org/10.1007/s007060170068.
[30] Y. Arslanoğlu, E. Hamuryudan, Synthesis and derivatization of near-IR absorbing titanylphthalocyanines with dimethylaminoethylsulfanyl substituents, Dyes Pigments 75 (2007) 150–155, https://doi.org/10.1016/j.dyepig.2006.05.019.
[31] Z. Bıyıklıoğlu, M. Durmuş, H. Kantekin, Tetra-2-[2-(dimethylamino)ethoxy]ethoxy substituted zinc phthalocyanines and their quaternized analogues: synthesis, characterization, photophysical and photochemical properties, J. Photochem. Photobiol. A Chem. 222 (2011) 87–96, https://doi.org/10.1016/j.jphotochem.2011.05.006.
[32] İ. Özçeşmeci, A.İ. Okur, A. Gül, New phthalocyanines bearing tetra (hydroxyethylthio) functionalities, Dyes Pigments 75 (2007) 761–765, https://doi.org/10.1016/j.dyepig.2006.08.003.
[33] M.N. Yaraşır, M. Kandaz, A. Koca, B. Salih, Polytopic cation receptor functional phthalocyanines: synthesis, characterization, electrochemistry and metal ion binding, Polyhedron 26 (2007) 1139–1147, https://doi.org/10.1016/j.poly.2006.10.002.
[34] S. Gümrükçü, E. Kaplan, T. Karazehir, M. Özçeşmeci, İ. Özçeşmeci, E. Hamuryudan, Reduced graphene oxide supported meso-pyridyl BODIPY-Cobaloxime complexes for electrocatalytic hydrogen evolution reaction, Int. J. Hydrog. Energy 89 (2024) 462–473, https://doi.org/10.1016/j.ijhydene.2024.09.284.
[35] Y. Yenilmez, Ö. Budak, N.F. Öztürk, A. Koca, A. Boz, B. Ustamehmetoğlu, Z. A. Bayır, Supercapacitive properties of carbazole-containing cobalt(ii) phthalocyanines/reduced graphene oxide composites, Dalton Trans. 53 (2024) 1766–1778, https://doi.org/10.1039/D3DT03602B.
[36] H. Du, R.C.A. Fuh, J. Li, L.A. Corkan, J.S. Lindsey, PhotochemCAD‡: a computer-aided design and research tool in photochemistry, Photochem. Photobiol. 68 (1998) 141–142, https://doi.org/10.1111/j.1751-1097.1998.tb02480.x.
[37] O. Osifeko, T. Nyokong, Synthesis and physicochemical properties of zinc and indium phthalocyanines conjugated to quantum dots, gold and magnetic nanoparticles, Dyes Pigments 131 (2016) 186–200, https://doi.org/10.1016/j.dyepig.2016.04.015.
[38] E. Gürel, M. Pişkin, S. Altun, Z. Odabaş, M. Durmuş, Synthesis, characterization and investigation of the photophysical and photochemical properties of highly soluble novel metal-free, zinc(ii), and indium(iii) phthalocyanines substituted with 2,3,6-trimethylphenoxy moieties, Dalton Trans. 44 (2015) 6202–6211, https://doi.org/10.1039/c5dt00304k.
[39] G.Y. Atmaca, N.K. Sabbagh, K. Celep, P. Şen, F. Şahin, A. Erdoğmuş, Enhanced singlet oxygen generation of zinc and indium phthalocyanines when conjugated to cysteine functionalized graphene quantum dots, J. Mol. Struct. 1340 (2025) 142583, https://doi.org/10.1016/j.molstruc.2025.142583.
[40] G. Wypych, Handbook of Antioxidants, 1st edition, ScienceDirect, 2020.
[41] M.S. Ağırtaş, İ. Gümüş, V. Okumus, A. Dundar, Design of Novel Binuclear Phthalocyanines formed by Dioxyphenyl bridges: synthesis and investigation of thermal and antioxidant properties, Z. Anorg. Allg. Chem. 638 (2012) 1868–1872, https://doi.org/10.1002/zaac.201200220.
[42] A.T. Bilgicli, Y. Tekin, E.H. Alici, M.N. Yaraşir, G. Arabaci, M. Kandaz, α- or β-substituted functional phthalocyanines bearing thiophen-3-ylmethanol substituents: synthesis, characterization, aggregation behavior and antioxidant activity, J. Coord. Chem. 68 (2015) 4102–4116, https://doi.org/10.1080/00958972.2015.1080361.
[43] G.P. Amaral, G.O. Puntel, C.L.D. Corte, F. Dobrachinski, R.P. Barcelos, L.L. Bastos, D.S. Ávila, J.B.T. Rocha, E.O. da Silva, R.L. Puntel, F.A.A. Soares, The antioxidant properties of different phthalocyanines, In Vitro Toxicol. 26 (2012) 125–132, https://doi.org/10.1016/j.tiv.2011.10.006.
[44] C. Kantar, B. Kaya, M. Türk, S. Şaşmaz, Novel phthalocyanines containing guaiacol azo dyes: synhthesis, antioxidant, antibacterial, and anticancer activity, J. Struct. Chem. 59 (2018) 1241–1250, https://doi.org/10.1134/S0022476618050335.
[45] K. Harmandar, E.N. Kaya, G. Tollu, İ.F. Sengul, S. Özdemir, D. Atilla, Synthesis, photo-physicochemical and biological properties of novel tetrahydropyrimidone-substituted metallo-phthalocyanines, Dalton Trans. 53 (2024) 16005–16017, https://doi.org/10.1039/D4DT02115K.
[46] K. Celep, G.Y. Atmaca, K. Eroğlu, P.D. Aydoğmuş, Ö.T. Günkara, G. Giray, G. Tollu, S. Özdemir, A. Erdoğmuş, Exploring improved strategies for therapeutic studies and biological activities of novel zinc and indium phthalocyanines, Dalton Trans. 53 (2024) 17381–17393, https://doi.org/10.1039/D4DT02261K.
[47] K. Huang, M. Yan, H. Zhang, J. Xue, J. Chen, A phthalocyanine-based photosensitizer for effectively combating triple negative breast cancer with enhanced photodynamic anticancer activity and immune response, Eur. J. Med. Chem. 241 (2022) 114644, https://doi.org/10.1016/j.ejmech.2022.114644.
[48] Y.-J. Zhu, J.-D. Huang, X.-J. Jiang, J.-C. Sun, Novel silicon phthalocyanines axially modified by morpholine: synthesis, complexation with serum protein and in vitro photodynamic activity, Inorg. Chem. Commun. 9 (2006) 473–477, https://doi.org/10.1016/j.inoche.2006.02.014.
[49] K. Li, L. Qiu, Q. Liu, G. Lv, X. Zhao, S. Wang, J. Lin, Conjugate of biotin with silicon (IV) phthalocyanine for tumor-targeting photodynamic therapy, J. Photochem. Photobiol. B Biol. 174 (2017) 243–250, https://doi.org/10.1016/j.jphotobiol.2017.08.003.
[50] K. Supruniuk, R. Czarnomysy, A. Muszyńska, I. Radziejewska, Anti-cancer effects of pyrazole-platinum(II) complexes combined with anti-MUC1 monoclonal antibody versus monotherapy in DLD-1 and HT-29 colon cancer cells, Transl. Oncol. 18 (2022) 101348, https://doi.org/10.1016/j.tranon.2022.101348.